molecules

MDPI

Article

Thermal Characterization and Heat Capacities of Seven Polyphenols

Iván Montenegro [1], Carmen Pérez [2], Begoña González [1], Ángeles Domínguez [1] and Elena Gómez [1,*]

[1] FEQx Lab, Department of Chemical Engineering, University of Vigo, 36310 Vigo, Spain; ivan.montenegro@uvigo.gal (I.M.); bgp@uvigo.es (B.G.); admguez@uvigo.es (Á.D.)
[2] CINTECX, ENCOMAT Group, University of Vigo, 36310 Vigo, Spain; cperez@uvigo.gal
* Correspondence: elenagc@uvigo.es

Abstract: Polyphenolic compounds are key elements in sectors such as pharmaceutics, cosmetics and food; thus, their physicochemical characterization is a vital task. In this work, the thermal behavior of seven polyphenols (*trans*-resveratrol, *trans*-polydatin, kaempferol, quercetin, myricetin, hesperidin, and (−)-epicatechin) was investigated with DSC (differential scanning calorimetry) and TGA (thermogravimetric analysis). Melting temperatures, enthalpies of fusion and decomposition temperatures were determined, and heat capacities were measured in the temperature range from 283.15 K to 363.15 K. Results were compared to the scarce experimental data available in the literature, showing a satisfactory agreement. All compounds were found to be thermally stable until melting, upon which they rapidly decomposed. Myricetin was the only polyphenol that presented polymorphic behavior, exhibiting two phase transitions prior to melting. Heat capacities increased minimally with temperature in the studied range. In addition, the group contribution method developed by Marrero and Gani was used to estimate the thermal properties of the polyphenols, achieving high accuracy for melting temperatures.

Keywords: polyphenols; DSC; TGA; heat capacity; enthalpy of fusion; decomposition

check for updates

Academic Editors: M. Gilles Mailhot and Leucio Rossi

Received: 2 December 2024
Revised: 26 December 2024
Accepted: 30 December 2024
Published: 6 January 2025

Citation: Montenegro, I.; Pérez, C.; González, B.; Domínguez, Á.; Gómez, E. Thermal Characterization and Heat Capacities of Seven Polyphenols. *Molecules* **2025**, *30*, 199. https://doi.org/10.3390/molecules30010199

Copyright: © 2025 by the authors. Licensee MDPI, Basel, Switzerland. This article is an open access article distributed under the terms and conditions of the Creative Commons Attribution (CC BY) license (https://creativecommons.org/licenses/by/4.0/).

1. Introduction

Polyphenols are bioactive compounds present in numerous plant species. The strong antioxidant character of these multifunctional molecules grants them anti-tumor, anti-inflammatory, cardio-protective, anti-aging, anti-cancer, and anti-microbial properties, among others [1–8]. Due to all these features, they have garnered considerable attention in relevant sectors such as food, cosmetics, medicine, bio- and nanotechnology and pharmaceutics [8–15], and thus numerous lines of research have focused on the study of polyphenols in the past decade. Specifically, the extraction of antioxidants from organic residues of fruits with high polyphenolic content—such as grapes and apples—is proving to be very promising due to its potential contribution to circular economy and waste revaluation [16–22].

Structurally, polyphenols can be divided into non-flavonoids (mainly stilbenes and phenolic acids) and flavonoids (flavanols, flavonols, flavanones, flavones, and anthocyanins). The latter can be further sub-classified depending on the saturation and oxidation degrees of the carbonic ring, and each of them has a glycoside form with an attached sugar molecule; in addition, different combinations of functional groups (kaempferol, quercetin, myricetin) and isomers (catechin and epicatechin) exist for a given polyphenolic sub-class [23]. As a result, the number of known polyphenols exceeds 8000 [24], thus representing a broad and complex field of research to cover.

Against this background, thermal characterization is essential for the comprehensive study of any compound. It provides crucial information about phase transitions, decomposition temperatures and thermal properties, e.g., melting points and enthalpies of fusion, which are indispensable for the optimal design of extraction and purification processes and fortified food treatment. In pharmaceutics, the thermal characterization of drugs allows the stability analysis and identification of compounds, as well as activity and purity determination and selection of packaging materials. In addition, heat capacities are required for physicochemical processing and calculation of thermodynamic potentials, which is necessary for thermodynamic modeling and analysis of multicomponent systems. Nevertheless, for most polyphenols, the study of these properties has been merely superficial so far.

Therefore, in this work, the thermal behavior of seven polyphenols was analyzed and their heat capacities in the solid state were determined from 283.15 K to 363.15 K. Melting points and enthalpies of fusion were obtained via differential scanning calorimetry (DSC), whereas decomposition temperatures were determined by thermogravimetric analysis (TG). The selection of compounds was carried out considering their concentration in plant species, the polyphenolic division and industrial application. This way, seven representative polyphenols of grape waste were studied [25] (chemical structures are displayed in Figure S1): two stilbenes (*trans*-resveratrol and *trans*-polydatin), three flavonols (kaempferol, quercetin, and myricetin), one flavanone (hesperidin), and one flavanol ((−)-epicatechin). Experimental melting temperatures and enthalpies of fusion were compared to the scarce literature data available and also to predicted values calculated by the group contribution method developed by Marrero and Gani [26] for thermal properties. As for heat capacities, no data were found except for quercetin.

2. Results and Discussion

2.1. Thermal Analysis

2.1.1. Experimental Results

The thermal behavior of seven polyphenols was evaluated using DSC and TG techniques. Figure 1 shows the DSC and TG curves of *trans*-resveratrol as an example (see Supplementary Information for the rest of curves), and experimental melting temperatures and enthalpies of fusion are included in Table 1, along with literature data for comparison. To perform the analysis, deviations from reference data are defined as follows:

$$\mathrm{ARD} = \left| \frac{X_{EXP,i} - X_{REF,j}}{X_{REF,j}} \right| \times 100 \quad (1)$$

$$\mathrm{AARD} = \left(\sum_{j=1}^{n} \left(\frac{X_{EXP,i} - X_{REF,j}}{X_{REF,j}} \right) \times 100 \right) \Big/ n \quad (2)$$

where ARD is the absolute relative deviation of any experimental magnitude $X_{EXP,i}$ determined in this work from any literature reference $X_{REF,j}$ for a given compound i, AARD is the average absolute relative deviation among j referenced values and n is the number of the selected literature references for each polyphenol.

All polyphenols proved to be thermally stable until melting, which is represented by a sharp endothermic peak for all compounds, indicating their crystalline nature. A clear exothermic peak is exhibited after melting in the DSC curves, which was accompanied by strong weight loss in the TG curves. This behavior could be associated with the degradation of the compounds. In the case of quercetin and hesperidin, this process took place immediately after the melting process, whereas *trans*-resveratrol and kaempferol (see Figure S3) remained stable around 60 K above their melting points, and so did *trans*-polydatin for almost 40 K after fusion. As for myricetin, melting and decomposition occurred almost si-

multaneously. The case of (−)-epicatechin stood out, as an exothermic peak did not appear, and vigorous degradation was observed after the fusion, representing the carbonization of the compound.

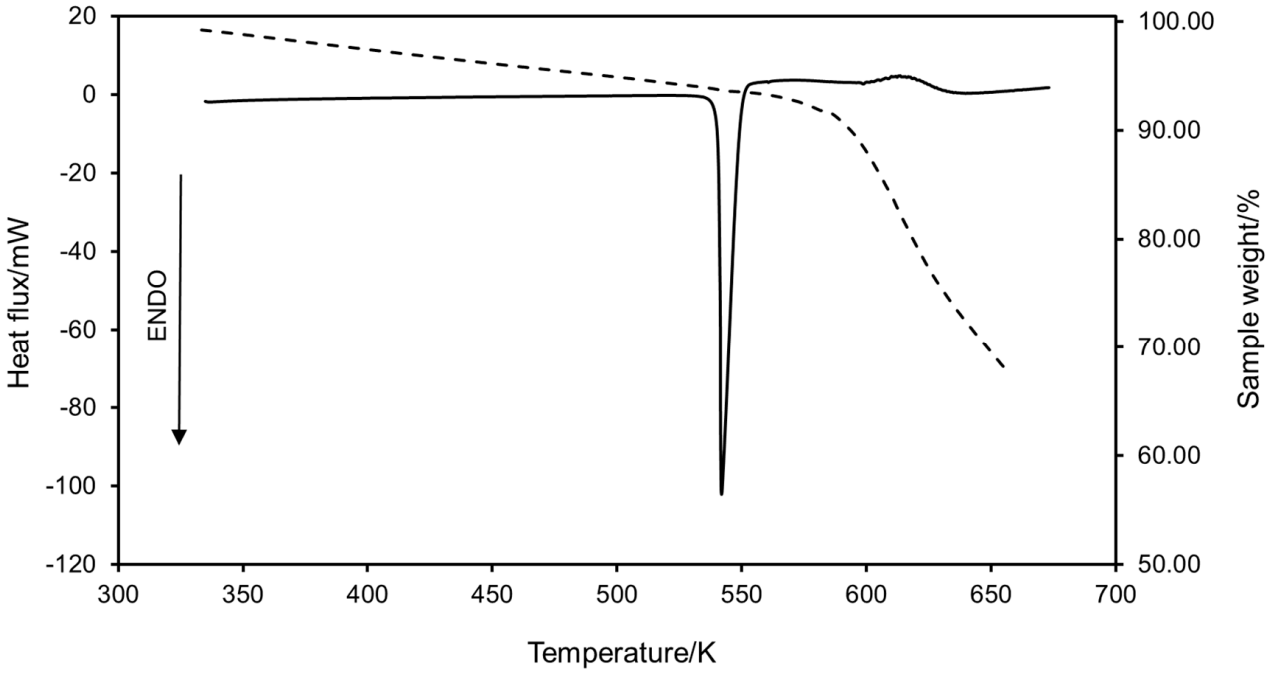

Figure 1. DSC (—) and TG (---) curves of *trans*-resveratrol.

A clear trend in the melting temperatures of flavonols was noticed, which increased with the number of hydroxyl groups present in the aromatic ring in the following order: kaempferol, quercetin, myricetin. In all cases, small weight loss, between 2 and 3% depending on the flavonol, was observed around 373 K, related to water evaporation. In addition, two solid–solid state transitions (SST) were identified for myricetin at T_{SST1} = 565.80 K (ΔH_{SST1} = 24.99 J·g^{-1}) and T_{SST2} = 612.15 K (ΔH_{SST2} = 4.19 J·g^{-1}), which had no associated mass loss. This polymorphic behavior was also reported in previous studies [27,28] and might be the cause of the shortened melting peak (see Figure S5) and abnormally low enthalpy of fusion of myricetin (ΔH_m = 81.26 J·g^{-1}) compared to those of the other two flavonols studied.

As for the melting temperatures, an excellent agreement with the scarce literature data was achieved in all cases. Maximum ARDs of 3.08%, 1.77%, and 1.52% were obtained for (−)-epicatechin, *trans*-polydatin, and myricetin, respectively, while for the rest of polyphenols, they only differ by up to 0.66%. Enthalpies of fusion are also very consistent with those previously reported, deviating 10.29%, 8.01%, and 1.47% on average (AARD) for hesperidin, (−)-epicatechin, and *trans*-resveratrol, respectively. Regarding kaempferol, a high discrepancy with the values obtained by Danciu et al. [29] was encountered, which was probably due to the small mass of the sample used for DSC in their study (mass = 2.53 mg). The melting enthalpy of quercetin is within the range of results obtained in the literature, and, to the best of our knowledge, no data were found for myricetin and *trans*-polydatin.

Table 1. Experimental melting temperatures, T_m, and enthalpies of fusion, ΔH_m, of the studied polyphenols, along with literature values.

Compound	T_m/K		ΔH_m/J·g^{-1}	
	Exp.	Ref.	Exp.	Ref.
Trans-resveratrol	541.95	541.25 [30], 542.25 [31], 541.66 [32]	294.53	303.20 [33], 293.6 [34], 298.2 [35]
Trans-polydatin	504.65	503.15 [36], 501.15 [37], 495.85 [38]	187.93	No data found
Kaempferol	557.51	558.15 [39], 561.23 [40], 560.15 [41]	163.68	34.45 [29]
Quercetin	596.49	596.15 [42], 596.15 [43], 596.25 [44]	176.96	155 [43], 206.6 [45], 115.37 [46]
Myricetin	638.75	646.15 [28], 641.15 [27], 629.21 [47]	81.26	No data found
Hesperidin	532.77	531.15 [42], 532.15 [48], 533.15 [49]	120.76	122 [42], 101.24 [50]
(−)-Epicatechin	524.84	512.15 [51], 520.32 [52], 509.15 [53]	150.78	139.6 [52]

Regarding the decomposition temperatures extracted from the TG curves, Table 2 shows the experimental values together with data from the literature. As with the melting temperatures, the values obtained are in agreement with the experimental references, with AARDs between 0.024% and 0.98% for *trans*-polydatin, myricetin, hesperidin, and (−)-epicatechin. Concerning *trans*-resveratrol and quercetin, higher discrepancies were noticed due to a remarkable divergence among the literature values, achieving AARDs of 2.70% and 7.28%, respectively. Kaempferol presents the highest deviation, with an 11.19% ARD with respect to the only one found in the literature, obtained by Cao et al. [54].

Table 2. Comparison of experimental decomposition temperatures (T_d) with referenced values.

Compound	T_d/K	
	Exp.	Ref.
Trans-resveratrol	593.25	511.45 [55], 546.15 [56], 563.75 [34]
Trans-polydatin	542.58	543.15.15 [57], 553.15 [58], 546.15 [37]
Kaempferol	631.97	561.25 [54]
Quercetin	623.58	609.15 [42], 594.15 [59], 617 [60]
Myricetin	633.30	633.15 [61]
Hesperidin	553.6	555.15 [42], 539.15 [54]
(−)-Epicatechin	524.84 [a]	521.15 K [52]

[a] Melting and decomposition occurred simultaneously.

2.1.2. Property Prediction by Group Contribution Method

The melting temperatures and enthalpies of fusion of the seven polyphenols were calculated by the group contribution method developed by Marreno and Gani [26], which has been widely employed for the estimation of thermal properties. The results are displayed in Table 3, as are the relative deviations from our experimental values regarding melting points (ARD_{Tm}) and enthalpies of fusion ($ARD_{\Delta Hm}$), which are redefined for this section, as shown in Equations (3) and (4):

$$ARD = \left| \frac{X_{GC,i} - X_{EXP,i}}{X_{EXP,i}} \right| \times 100 \quad (3)$$

$$AARD = \left(\sum_{i=1}^{n} \left(\frac{X_{GC,i} - X_{EXP,i}}{X_{EXP,i}} \right) \times 100 \right) \Big/ n \quad (4)$$

where $X_{GC,i}$ refers to a thermal property of a certain polyphenol i, estimated with the group contribution method provided by Marreno and Gani [26], while n indicates the number of polyphenols.

Table 3. Comparison of experimental melting points and enthalpies of fusion (T_m, ΔH_m) and those calculated by the group contribution method developed by Marrero and Gani [26] ($T_{m,GC}$, $\Delta H_{m,G.C}$).

Compound	T_m/K	$T_{m,GC}$/K	ARD_{Tm}/%	ΔH_m/J·g^{-1}	$\Delta H_{m,GC}$/J·g^{-1}	$ARD_{\Delta Hm}$/%
Trans-resveratrol	541.95	486.89	10.16	294.53	201.52	31.58
Trans-polydatin	504.65	525.15	4.06	187.93	194.03	3.24
Kaempferol	557.51	525.40	5.76	163.68	145.78	10.93
Quercetin	596.49	538.24	9.77	176.96	154.39	12.76
Myricetin	638.75	557.55	12.71	81.26	160.88	97.98
Hesperidin	532.77	582.71	9.37	120.76	159.35	31.96
(−)-Epicatechin	524.84	512.01	2.44	150.78	170.56	13.12

The resulting AARD for melting temperatures is 9.05%, denoting an adequate estimation. Predicted values diverge by less than 5% from experimental results for *trans*-polydatin and (−)-epicatechin and up to 10% for kaempferol, hesperidin, and quercetin. On the contrary, for *trans*-resveratrol and myricetin, this threshold is slightly exceeded. Regarding flavonols, it is also observed that the ARDs in the experimental values increase with the molecular weight, i.e., with the number of hydroxyl groups present in the aromatic rings. This fact highlights the influence of the position of the hydroxyl group in the benzene ring, which is not considered in the group contribution method applied. As for the enthalpy of fusion, the best estimation was again achieved for *trans*-polydatin, this being below 5% of ARD, whilst moderate discrepancies (<14%) were obtained for kaempferol, quercetin, and (−)-epicatechin. The accuracy of the method was insufficient for *trans*-resveratrol, hesperidin, and myricetin, with the latter achieving the greatest ARD compared to our experimental results. This is probably due to the near-fusion polymorphism of the compound, a phenomenon not accounted for by the group contribution method, and is probably the reason why deviations are remarkably lower for the other two flavonols.

2.2. Heat Capacities

The heat capacities of the seven compounds were measured via DSC following the sapphire method in a three-stage program from 273.15 K to 373.15 K. Values below 283.15 K and above 363.15 K were discarded for accuracy reasons. Results in 10 K steps are plotted in Figures 2 and 3, and were linearly fitted by Equation (5):

$$c_p = y_0 + a \times T(K) \quad (5)$$

where c_p is the heat capacity in J·g^{-1}·K^{-1}, and y_0 and a are fitting coefficients. The latter, along with the R^2 values obtained from the regression, are collected in Table 4 for each polyphenol. Although the calculation of heat capacities was performed on a mass basis (J·g^{-1}·K^{-1}) as dictated by the procedure, molar heat capacities (J·mol^{-1}·K^{-1}) are displayed in Figures 2 and 3 for purely comparative purposes, since this property is roughly additive and molar values are recommended for the analysis regarding structural features of the polyphenols.

Slight increases with temperature are observed for all compounds in the range studied, the most notorious being for trans-polydatin (28.31%) and the least being for quercetin (22.39%), although slopes from the fitting are quite similar in all cases. Hesperidin achieved higher heat capacities in the whole temperature range than any other polyphenol, with a maximum of 665.66 J·mol^{-1}·K^{-1} at 363.15 K, while the minimum corresponds to *trans*-resveratrol, with 183.66 J·mol^{-1} K^{-1} at the lowest temperature. This highlights the trend of the molar heat capacities with the molecular weight of the compounds, as the heavier the compound, the higher the molar heat capacity, following the order: hesperidin > *trans*-polydatin > myricetin > (−)-epicatechin ≅ kaempferol > *trans*-resveratrol. Quercetin is the

only compound that does not follow the trend, differing with *trans*-resveratrol by 1.09% on average in the studied range. As for (−)-epicatechin and kaempferol, they differ by only 2.37% on average in the whole temperature range, which is in agreement with their almost equal molecular weights (290.27 g·mol^{-1} and 286.24 g·mol^{-1}, respectively).

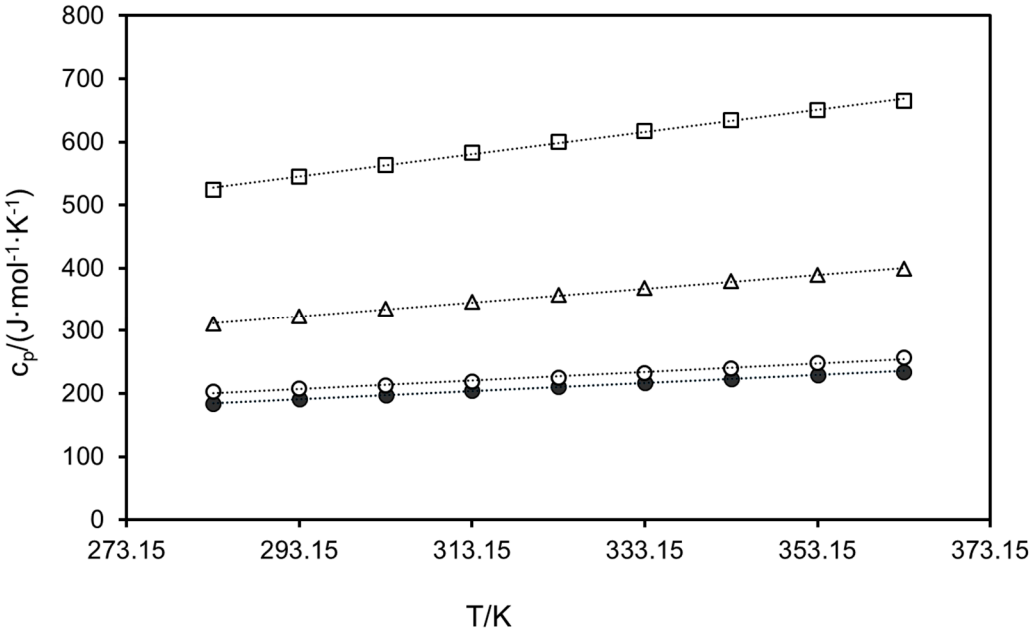

Figure 2. Experimental molar heat capacities of (●) *trans*-resveratrol, (△) *trans*-polydatin, (□) hesperidin, and (○) (−)-epicatechin. Dotted lines are depicted for better trend visualization.

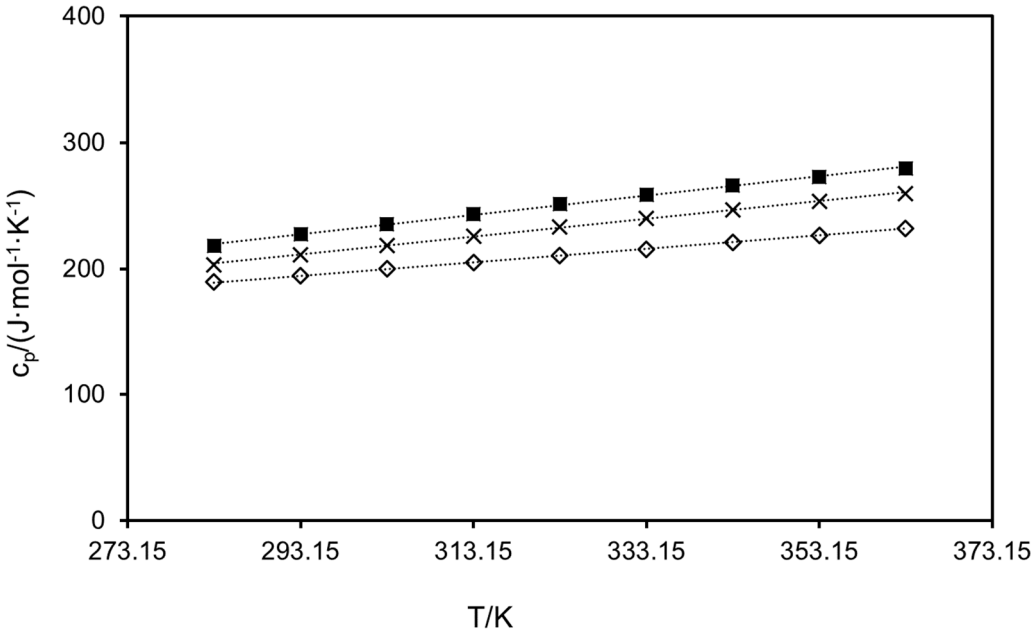

Figure 3. Experimental molar heat capacities of (×) kaempferol, (◇) quercetin, and (■) myricetin. Dotted lines are depicted for better trend visualization.

As far as stilbenes are concerned, the molar heat capacities of *trans*-polydatin are 1.70 times higher than those of *trans*-resveratrol from 283.15 K to 363.15 K, revealing the influence of the glucose molecule in the chemical species. Contrary to the melting temperatures, no trend was observed in Figure 3 regarding the number of hydroxyl groups of the flavonols; thus, kaempferol heat capacities were from 6.95% to 11.70% higher than those of quercetin in the temperature range studied, whereas values of myricetin exceeded

those of kaempferol by 7.72% on average. These discrepancies emphasize that not only does the number of the hydroxyl group in the benzene ring influence the heat capacity, but so does its position.

Table 4. Fitting parameters of the linear regression of experimental c_p ($J \cdot g^{-1} \cdot K^{-1}$).

Compound	y_0	$a \cdot 10^3$	R^2
Trans-resveratrol	0.0181	2.80	0.998
Trans-polydatin	0.0038	2.81	0.998
Kaempferol	0.0158	2.46	0.998
Quercetin	0.1305	1.75	0.999
Myricetin	0.0134	2.39	0.998
Hesperidin	0.0456	2.89	0.998
(−)-Epicatechin	0.0318	2.33	0.990

No experimental data were found in the literature for any polyphenol except for quercetin. Li et al. [62] measured the heat capacity of pure quercetin from 298.2 K to 470.2 K. They also applied the three-step method with DSC, employing sapphire as the reference substance. However, they used a remarkably lower sample mass than we did (of about 5 mg, whereas the recommended amount is ten times higher), and a heating rate of 5 K min^{-1} for the dynamic segment. Average deviations of 44.45% were obtained with respect to their values in the temperature range from 298.2 K to 363.2 K.

3. Materials and Methods

3.1. Materials

Detailed information about the polyphenols used in this study is reported in Table 5. All of them were dried in situ before each experiment.

Table 5. Information of materials used for experimentation.

Compound	CAS Number	Source	Molecular Weight/$g \cdot mol^{-1}$	Mass Purity [a]/%
Trans-resveratrol	501-36-0	TCI	228.24	>99.0
Trans-polydatin	65914-17-2	Sigma-Aldrich	390.38	≥95
Kaempferol	520-18-3	Apollo Scientific	286.24	98
Quercetin	117-39-5	Sigma-Aldrich	302.24	≥95
Myricetin	529-44-2	Sigma-Aldrich	318.24	>97.0
Hesperidin	520-26-3	Supelco	610.57	≥99.9
(−)-Epicatechin	490-46-0	TCI	290.27	≥97.0

[a] Provided by the supplier.

3.2. Methods

3.2.1. Thermal Analysis

Melting Point and Enthalpy of Fusion

Thermal profiles of all polyphenols were determined by differential scanning calorimetry using a Mettler Toledo 822e/400 DSC apparatus. Samples of 4 to 12 mg were weighted on an AX-205 DeltaRange balance from Mettler Toledo (Columbus, OH, USA) and placed in 40 µL aluminum crucibles with a pinhole. Measurements were carried out covering the melting of all compounds as follows: performing dynamic heating from 298.15 K to 673.15 K at a heating rate of 10 $K \cdot min^{-1}$, with previous drying at 393.15 K for 15 min. Inert atmosphere was maintain throughout the whole study with a 50 $mL \cdot min^{-1}$ constant flow of nitrogen. Melting temperatures were considered the endothermic peaks of the DSC curves, whereas enthalpies of fusion were directly integrated with the apparatus software STAR^e SW 16.10. Experiments were performed in duplicate for each polyphenol.

Calibration for temperature and heat flow was performed using pure zinc, indium, water, and heptane, with a repeatability in the enthalpy of fusion of ±2% and in the temperature of ±0.2%. To estimate the uncertainty in the measurement of temperature, a pure-indium sample (provided by Mettler Toledo) was used. The following variables were taken into account:

(i) Uncertainty of apparatus: Three replicate scans of the same sample were completed in the furnace. This uncertainty was found to be ±0.03 K for melting temperature and ±0.5 $J \cdot g^{-1}$ for enthalpy of fusion.

(ii) Uncertainty of the operator and positioning in the furnace: Two different operators removed and replaced the sample three times each. The uncertainty was ±0.35 K for melting temperature and ±1.5 $J \cdot g^{-1}$ for enthalpy of fusion.

(iii) Uncertainty of sample and pan: A new pan with pure indium was used. This uncertainty was found to be ±0.05 K for melting temperature and ±0.6 $J \cdot g^{-1}$ for enthalpy of fusion.

Finally, in this work, the standard uncertainty in the measurement of the temperature and in the enthalpy of fusion were assumed to be ±1 K for melting temperature and ±2 $J \cdot g^{-1}$ for enthalpy of fusion, since the phase transition temperature can depend on other variables, such as the heating and cooling rate.

3.2.2. Heat Capacity

The classical three-step procedure [63] was chosen for heat capacity determination using DSC, employing sapphire (ref. ME-51140818) as the reference substance. It consisted of three segments: the first isothermal period at 273.15 K for 15 min, followed by dynamic heating to 373.15 K at 10 $K \cdot min^{-1}$, and ending with a final isothermal segment for other 15 min at 373.15 K. Pre-drying was performed at 393.15 K for 15 min. A constant nitrogen flow of 50 $mL \cdot min^{-1}$ was supplied to the furnace. Since this is a comparative procedure, a higher amount of sample (≅50 mg) was necessary for each experiment, as the measurement signal provided by both the sapphire and the sample must be clear and sufficiently close to attain high accuracy [64]. An AX-205 DeltaRange balance from Mettler Toledo was again used for the weighting process for the samples. Measurements were performed in duplicate for each polyphenol.

To calculate the uncertainty in the measurement of heat capacity, a pure sapphire sample (supplied by Mettler Toledo) was used. The same variables for the estimation of the uncertainty in the measurement of temperature and enthalpy of fusion were taken into account:

(i) Uncertainty of apparatus: This uncertainty was found to be ±0.00013 $J \cdot K^{-1} \cdot g^{-1}$.

(ii) Uncertainty of the operator and positioning in the furnace: This uncertainty was ±0.0035 $J \cdot K^{-1} \cdot g^{-1}$.

(iii) Uncertainty of sample and pan: A new pan with pure sapphire was used; this uncertainty was found to be ±0.0015 $J \cdot K^{-1} \cdot g^{-1}$.

In this case, taking into account the influence of the uncertainty of the mass of the sample and of the sapphire reference on the overall uncertainty of the measurement of heat capacity, the standard uncertainty was estimated to be ±0.006 $J \cdot K^{-1} \cdot g^{-1}$.

3.2.3. Thermogravimetric Analysis

TG measurements were carried out using a Mettler Toledo TGA/DSC1 instrument. Compounds were used as supplied, with no purification method applied. Powder samples, between 9 and 20 mg in weight, were placed in 40 µL pinhole aluminum crucibles. They were heated from 298 K to 723 K at a heating rate of 10 $K \cdot min^{-1}$, and a nitrogen stream with a flow of 50 $mL \cdot min^{-1}$ was used. Decomposition temperatures were considered the

onset of the TG curves, from which the mass lost was considerable. This procedure was carried out in duplicate for each polyphenol.

4. Conclusions

The thermal behavior of seven polyphenols present in plant waste was investigated through DSC and TGA. Melting points, enthalpies of fusion, and decomposition temperatures were determined, and heat capacities were calculated from 283.15 K to 363.15 K; none had been reported so far in the literature for most compounds studied.

All compounds proved to be thermally stable until fusion, upon which decomposition started. Myricetin stands out for being the only polyphenol that shows polymorphic behavior, exhibiting two solid–solid transitions close to melting. Good agreement with the literature values was observed, despite the scarce experimental data available. In addition, the group contribution method developed by Marrero and Gani [26] was used to predict the thermal properties of the polyphenols, having been proven to be able to estimate the melting temperatures of all compounds with high accuracy. In addition, heat capacities showed a slight increase with temperature in the range studied for all cases, and a clear upward trend with the molecular weight was observed for this thermophysical property in all polyphenols except for quercetin.

Supplementary Materials: The following supporting information can be downloaded at: https://www.mdpi.com/article/10.3390/molecules30010199/s1. Figure S1: Chemical structure of *trans*-resveratrol (a), *trans*-polydatin (b), kaempferol (c), quercetin (d), myricetin (e), (−)-epicatechin (f), and hesperidin (g). Figure S2: DSC (—) and TG (---) curves of *trans*-polydatin. Figure S3: DSC (—) and TG (---) curves of kaempferol. Figure S4: DSC (—) and TG (---) curves of quercetin. Figure S5: DSC (—) and TG (---) curves of myricetin. Figure S6: DSC (—) and TG (---) curves of hesperidin. Figure S7: DSC (—) and TG (---) curves of (-)-epicatechin.

Author Contributions: E.G., B.G. and Á.D. contributed to the study's conception and supervision. Material preparation, investigation, data collection and analysis were performed by I.M. and C.P. The first draft of the manuscript was written by I.M. and C.P. and all authors commented on the following versions of the manuscript. All authors have read and agreed to the published version of the manuscript.

Funding: This work was supported by Xunta de Galicia (GPC-ED431B 2020/08). Elena Gómez gives thanks for the funding support from María Zambrano Grants for the Attraction of International Talent from the Spanish Ministry of Universities and Iván Montenegro is grateful to Xunta de Galicia (Consellería de Educación, Ciencia, Universidades e FP) for his predoctoral grant (ED481A-2024-022), which is also co-financed by the European Unión within the framework of Programa FSE+ Galicia 2021–2027.

Data Availability Statement: Data are contained within the article or Supplementary Material. The original contributions presented in this study are included in the article/Supplementary Material. Further inquiries can be directed to the corresponding authors.

Acknowledgments: This work was supported by Xunta de Galicia (GPC-ED431B 2020/08). Elena Gómez gives thanks for the funding support from María Zambrano Grants for the Attraction of International Talent from the Spanish Ministry of Universities and Iván Montenegro is grateful to Xunta de Galicia (Consellería de Educación, Ciencia, Universidades e FP) for his predoctoral grant (ED481A-2024-022), which is also co-financed by the European Unión within the framework of Programa FSE+ Galicia 2021–2027.

Conflicts of Interest: The authors declare no conflicts of interest.

References

1. Ashrafizaveh, S.; Ashrafizadeh, M.; Zarrabi, A.; Husmandi, K.; Zabolian, A.; Shahinozzaman, M.; Aref, A.R.; Hamblin, M.R.; Nabavi, N.; Crea, F.; et al. Long non-coding RNAs in the doxorubicin resistance of cancer cells. *Cancer Lett.* **2021**, *508*, 104–114. [CrossRef] [PubMed]
2. Joy, A.T.; Harish, M.; Rishad, K.S. Anti-Inflammatory Activity of Phytoconstituents of Ginseng Plant—Insilico Approach. *Biomed. Pharmacol. J.* **2023**, *16*, 1179–1188. [CrossRef]
3. Aliaño-González, M.J.; Gabaston, J.; Ortiz-Somovilla, V.; Cantos-Villar, E. Wood Waste from Fruit Trees: Biomolecules and Their Applications in Agri-Food Industry. *Biomolecules* **2022**, *12*, 238. [CrossRef] [PubMed]
4. Auguste, S.; Yan, B.; Magina, R.; Xue, L.; Neto, C.; Guo, M. Cranberry extracts and cranberry polyphenols induce mitophagy in human fibroblast cells. *Food Biosci.* **2023**, *57*, 103549. [CrossRef]
5. Li, W.; Chen, H.; Xu, B.; Wang, Y.; Zhang, C.; Cao, Y.; Xing, X. Research progress on classification, sources and functions of dietary polyphenols for prevention and treatment of chronic diseases. *J. Future Foods* **2023**, *3*, 289–305. [CrossRef]
6. Abotaleb, M.; Samuel, S.M.; Varghese, E.; Varghese, S.; Kubatka, P.; Liskova, A.; Büsselberg, D. Flavonoids in cancer and apoptosis. *Cancers* **2019**, *11*, 28. [CrossRef] [PubMed]
7. Poveda, J.M.; Loarce, L.; Alarcón, M.; Díaz-Maroto, M.C.; Alañón, M.E. Revalorization of winery by-products as source of natural preservatives obtained by means of green extraction techniques. *Ind. Crops Prod.* **2018**, *112*, 617–625. [CrossRef]
8. Russo, G.L.; Spagnuolo, C.; Russo, M.; Tedesco, I.; Moccia, S.; Cervellera, C. Mechanisms of aging and potential role of selected polyphenols in extending healthspan. *Biochem. Pharmacol. Inc.* **2020**, *173*, 113719. [CrossRef]
9. Trujillo-Mayol, I.; Sobral, M.M.C.; Viegas, O.; Cunha, S.C.; Alarcón-Enos, J.; Pinho, O.; Ferreira, I.M. Incorporation of avocado peel extract to reduce cooking-induced hazards in beef and soy burgers: A clean label ingredient. *Food Res. Int.* **2021**, *147*, 110434. [CrossRef]
10. López-Pedrouso, M.; Lorenzo, J.M.; Franco, D. Advances in Natural Antioxidants for Food Improvement. *Antioxidants* **2022**, *11*, 1825. [CrossRef]
11. Pinela, J.; Prieto, M.; Barreiro, M.F.; Carvalho, A.M.; Oliveira, M.B.P.; Curran, T.P.; Ferreira, I.C. Valorisation of tomato wastes for development of nutrient-rich antioxidant ingredients: A sustainable approach towards the needs of the today's society. *Innov. Food Sci. Emerg. Technol.* **2017**, *41*, 160–171. [CrossRef]
12. Montagner, G.E.; Wingert, N.R.; Stein, C.d.S.; Moresco, R.N.; Fogaça, A.d.O.; Gomes, P. Optimization of the extraction of antioxidant compounds from grape seed from winemaking waste. *Sustain. Chem. Pharm.* **2022**, *30*, 100856. [CrossRef]
13. Ghasemzadeh, A.; Baghdadi, A.; Jaafar, H.Z.E.; Swamy, M.K.; Megat Wahab, P.E. Optimization of flavonoid extraction from red and brown rice bran and evaluation of the antioxidant properties. *Molecules* **2018**, *23*, 1863. [CrossRef] [PubMed]
14. Kumar, M.; Dahuja, A.; Sachdev, A.; Tomar, M.; Lorenzo, J.M.; Dhumal, S.; Radha, M.; Chandran, D.; Varghese, E.; Saha, S.; et al. Optimization of the use of cellulolytic enzyme preparation for the extraction of health promoting anthocyanins from black carrot using response surface methodology. *LWT* **2022**, *163*, 113528. [CrossRef]
15. Gómez-Mejía, E.; Vicente-Zurdo, D.; Rosales-Conrado, N.; León-González, M.E.; Madrid, Y. Screening the extraction process of phenolic compounds from pressed grape seed residue: Towards an integrated and sustainable management of viticultural waste. *LWT* **2022**, *169*, 113988. [CrossRef]
16. Zentelis, A.D.; Kodjapashis, M.P.; Kotrotsos, N.; Zagklis, D.P.; Sygouni, V.; Lamari, F.N.; Paraskeva, C.A. Separation, Isolation, and Enrichment of Samples of Phenolic Compounds from Winemaking By-Products. *Sustainability* **2023**, *15*, 12221. [CrossRef]
17. Fernandez, A.; Sette, P.; Echegaray, M.; Soria, J.; Salvatori, D.; Mazza, G.; Rodriguez, R. Clean recovery of phenolic compounds, pyro-gasification thermokinetics, and bioenergy potential of spent agro-industrial bio-wastes. *Biomass. Convers. Biorefin.* **2023**, *13*, 12509–12526. [CrossRef]
18. Pollini, L.; Blasi, F.; Ianni, F.; Grispoldi, L.; Moretti, S.; Di Veroli, A.; Cossignani, L.; Cenci-Goga, B.T. Ultrasound-Assisted Extraction and Characterization of Polyphenols from Apple Pomace, Functional Ingredients for Beef Burger Fortification. *Molecules* **2022**, *27*, 1993. [CrossRef]
19. Vorobyova, V.; Vasyliev, G.; Skiba, M.; Frolenkova, S.; Zaporozhets, J.; Gnatko, O.; Linyucheva, O. Green extraction of phenolic compounds from grape pomace by deep eutectic solvent extraction: Physicochemical properties, antioxidant capacity. *Chem. Pap.* **2023**, *77*, 2447–2458. [CrossRef]
20. Mattonai, M.; Massai, P.; Ribechini, E. Sustainable microwave-assisted eutectic solvent extraction of polyphenols from vine pruning residues. *Microchem. J.* **2024**, *197*, 109816. [CrossRef]
21. Hobbi, P.; Okoro, O.V.; Hajiabbas, M.; Hamidi, M.; Nie, L.; Megalizzi, V.; Musonge, P.; Dodi, G.; Shavandi, A. Chemical Composition, Antioxidant Activity and Cytocompatibility of Polyphenolic Compounds Extracted from Food Industry Apple Waste: Potential in Biomedical Application. *Molecules* **2023**, *28*, 675. [CrossRef] [PubMed]
22. Caldas, T.W.; Mazza, K.E.L.; Teles, A.S.C.; Mattos, G.N.; Brígida, A.I.S.; Conte-Junior, C.A.; Borguini, R.G.; Godoy, R.L.O.; Cabral, L.M.C.; Tonon, R.V. Phenolic compounds recovery from grape skin using conventional and non-conventional extraction methods. *Ind. Crops. Prod.* **2018**, *111*, 86–91. [CrossRef]

23. Panche, A.N.; Diwan, A.D.; Chandra, S.R. Flavonoids: An overview. *J. Nutr. Sci.* **2016**, *5*, 5–15. [CrossRef] [PubMed]
24. Patel, K.; Patel, D.K. Medicinal Importance and Therapeutic Benefit of Bioactive Flavonoid Eriocitrin: An Update on Pharmacological Activity and Analytical Aspects. *Nat. Prod. J.* **2024**, *14*, 2. [CrossRef]
25. Brezoiu, A.-M.; Matei, C.; Deaconu, M.; Stanciuc, A.-M.; Trifan, A.; Gaspar-Pintiliescu, A.; Berger, D. Polyphenols extract from grape pomace. Characterization and valorisation through encapsulation into mesoporous silica-type matrices. *Food Chem. Toxicol.* **2019**, *133*, 110787. [CrossRef]
26. Marrero, J.; Gani, R. Group-contribution based estimation of pure component properties. *Fluid Phase Equilib.* **2001**, *183–184*, 183–208. [CrossRef]
27. Franklin, S.J.; Myrdal, P.B. Solid-State and Solution Characterization of Myricetin. *AAPS PharmSciTech* **2015**, *16*, 1400–1408. [CrossRef] [PubMed]
28. Yan, T.; Tao, Y.; Wang, X.; Lv, C.; Miao, G.; Wang, S.; Wang, D.; Wang, Z. Preparation, characterization and evaluation of the antioxidant capacity and antitumor activity of myricetin microparticles formated by supercritical antisolvent technology. *J. Supercrit. Fluids* **2021**, *175*, 105290. [CrossRef]
29. Corina, D.; Bojin, F.; Ambrus, R.; Muntean, D.; Soica, C.; Paunescu, V.; Cristea, M.; Pinzaru, I.; Dehelean, C. Physico-chemical and Biological Evaluation of Flavonols: Fisetin, Quercetin and Kaempferol Alone and Incorporated in beta Cyclodextrins. *Anti-Cancer Agents Med. Chem.* **2017**, *17*, 615–626. [CrossRef]
30. Zhao, Z.; Xiong, W.; Ju, X.; Yao, Y.; Zhang, J.; Wang, L. Fabrication and Characterization of Resveratrol-Loaded Gliadin Particles Stabilized by Gelatin. *Food Biophys.* **2023**, *18*, 510–519. [CrossRef]
31. Xie, X.; Jin, X.; Huang, J.; Yi, J.; Li, X.; Huang, Z.; Lin, Q.; Guo, B. High resveratrol-loaded microcapsules with trehalose and OSA starch as the wall materials: Fabrication, characterization, and evaluation. *Int. J. Biol. Macromol.* **2023**, *242*, 124825. [CrossRef] [PubMed]
32. Yang, X.; Shen, J.; Liu, J.; Yang, Y.; Hu, A.; Ren, N.; Cheng, Z.; Liu, W. Spray-Drying of Hydroxypropyl β-Cyclodextrin Microcapsules for Co-Encapsulation of Resveratrol and Piperine with Enhanced Solubility. *Crystals* **2022**, *12*, 596. [CrossRef]
33. Bhatt, P.; Fnu, G.; Bhatia, D.; Shahid, A.; Sutariya, V. Nanodelivery of Resveratrol-Loaded PLGA Nanoparticles for Age-Related Macular Degeneration. *AAPS PharmSciTech* **2020**, *21*, 291. [CrossRef] [PubMed]
34. Zhou, Z.; Li, W.; Sun, W.-J.; Lu, T.; Tong, H.H.; Sun, C.C.; Zheng, Y. Resveratrol cocrystals with enhanced solubility and tabletability. *Int. J. Pharm.* **2016**, *509*, 391–399. [CrossRef] [PubMed]
35. Zhang, X.P.; Le, Y.; Wang, J.X.; Zhao, H.; Chen, J.F. Resveratrol nanodispersion with high stability and dissolution rate. *LWT* **2013**, *50*, 622–628. [CrossRef]
36. Li, S.; Yuan, L.; Zhang, B.; Zhou, W.; Wang, X.; Bai, D. Photostability and antioxidant activity studies on the inclusion complexes of: Trans -polydatin with β-cyclodextrin and derivatives. *RSC Adv.* **2018**, *8*, 25941–25948. [CrossRef] [PubMed]
37. Zhang, J.Q.; Jiang, K.M.; Xie, X.G.; Jin, Y.; Lin, J. Water-soluble inclusion complexes of trans-polydatin by cyclodextrin complexation: Preparation, characterization and bioactivity evaluation. *J. Mol. Liq.* **2016**, *219*, 592–598. [CrossRef]
38. Kang, M.; Du, D.; Zhang, S.; Zhang, S.; Li, Z.; Dongye, Z.; Wang, L.; Qian, Y.; Chen, C.; Cheng, X.; et al. Non-covalent Complexes Between β-lactoglobulin and Baicalein: Characteristics and Binding Properties. *Food Biophys.* **2024**, *19*, 58–70. [CrossRef]
39. Raghav, S.S.; Kumar, B.; Sethiya, N.K.; Pahwa, S. Development and optimization of kaempferol loaded ethosomes using Box–Behnken statistical design: In vitro and ex-vivo assessments. *J. Biomed. Mater. Res. B Appl. Biomater.* **2024**, *112*, e35394. [CrossRef] [PubMed]
40. Zhou, H.; Duan, C.; Qin, H.; Huang, C.; Hou, J.; Chen, Y.; Zhu, J.; Xu, C.; Jin, J.; Zhuang, T. Synthesis and structural characterization of a novel palbociclib-kaempferol cocrystal with improved tabletability and synergistic antitumor activity. *J. Mol. Struct.* **2023**, *1281*, 135101. [CrossRef]
41. Colombo, M.; Melchiades, G.d.L.; Michels, L.R.; Figueiró, F.; Bassani, V.L.; Teixeira, H.F.; Koester, L.S. Solid Dispersion of Kaempferol: Formulation Development, Characterization, and Oral Bioavailability Assessment. *AAPS PharmSciTech.* **2019**, *20*, 106. [CrossRef]
42. Krekora, M.; Markiewicz, K.H.; Wilczewska, A.Z.; Nawrocka, A. Raman and thermal (TGA and DSC) studies of gluten proteins supplemented with flavonoids and their glycosides. *J. Cereal Sci.* **2023**, *111*, 103672. [CrossRef]
43. Wang, L.; Li, S.; Xu, X.; Xu, X.; Wang, Q.; Li, D.; Zhang, H. Drug-drug cocrystals of theophylline with quercetin. *J. Drug Deliv. Sci. Technol.* **2022**, *70*, 103228. [CrossRef]
44. Han, J.; Tong, M.; Li, S.; Yu, X.; Hu, Z.; Zhang, Q.; Xu, R.; Wang, J. Surfactant-free amorphous solid dispersion with high dissolution for bioavailability enhancement of hydrophobic drugs: A case of quercetin. *Drug Dev. Ind. Pharm.* **2021**, *47*, 153–162. [CrossRef]
45. Alhajj, N.; O'Reilly, N.J.; Cathcart, H. Development and characterization of a spray-dried inhalable ciprofloxacin-quercetin co-amorphous system. *Int. J. Pharm.* **2022**, *618*, 121657. [CrossRef] [PubMed]

46. Manta, K.; Papakyriakopoulou, P.; Chountoulesi, M.; Diamantis, D.A.; Spaneas, D.; Vakali, V.; Naziris, N.; Chatziathanasiadou, M.V.; Andreadelis, I.; Moschovou, K.; et al. Preparation and Biophysical Characterization of Quercetin Inclusion Complexes with β-Cyclodextrin Derivatives to be Formulated as Possible Nose-to-Brain Quercetin Delivery Systems. *Mol. Pharm.* **2020**, *17*, 4241–4255. [CrossRef]
47. Hong, C.; Xie, Y.; Yao, Y.; Li, G.; Yuan, X.; Shen, H. A Novel strategy for pharmaceutical cocrystal generation without knowledge of stoichiometric ratio: Myricetin cocrystals and a ternary phase diagram. *Pharm. Res.* **2015**, *32*, 47–60. [CrossRef] [PubMed]
48. Rosiak, N.; Wdowiak, K.; Tykarska, E.; Cielecka-Piontek, J. Amorphous Solid Dispersion of Hesperidin with Polymer Excipients for Enhanced Apparent Solubility as a More Effective Approach to the Treatment of Civilization Diseases. *Int. J. Mol. Sci.* **2022**, *23*, 15198. [CrossRef] [PubMed]
49. Afkhami, R.; Goli, M.; Keramat, J. Loading lime by-product into derivative cellulose carrier for food enrichment. *Food Sci. Nutr.* **2019**, *7*, 2353–2360. [CrossRef]
50. Joshi, S.; Dhingra, A.K.; Chopra, B.; Dass, R.; Guarve, K.; Sapra, S. Formulation and Evaluation of Solid Dispersions of Poorly Water-Soluble Drug-Hesperidin. *Lett. Appl. NanoBioSci.* **2023**, *12*, 50. [CrossRef]
51. Kim, J.S. Study of flavonoid/hydroxypropyl-β;-cyclodextrin inclusion complexes by UV-Vis, FT-IR, DSC, and X-Ray diffraction analysis. *Prev. Nutr. Food Sci.* **2020**, *25*, 449–456. [CrossRef] [PubMed]
52. Álvarez, C.M.; Restrepo-Uribe, L.; López, J.A.; Estrada, O.A.; Noriega, M.D.P. Improvement of stability and release of (-)-epicatechin by hot melt extrusion. *J. Pol. Eng.* **2020**, *40*, 75–85. [CrossRef]
53. Shi, J.; Yu, J.; Pohorly, J.E.; Kakuda, Y. Polyphenolics in Grape Seeds-Biochemistry and Functionality. *J. Med. Food.* **2003**, *6*, 291–299. [CrossRef] [PubMed]
54. Cao, R.; Zhao, Y.; Zhou, Z.; Zhao, X. Enhancement of the water solubility and antioxidant activity of hesperidin by chitooligosaccharide. *J. Sci. Food Agric.* **2018**, *98*, 2422–2427. [CrossRef] [PubMed]
55. Freire, T.B.; Castro Lima CRR de Oliveira Pinto CAS de Borge, L.F.; Baby, A.R.; Velasco, M.V.R. Evaluation of interaction between natural antioxidants and chemical sunscreens aiming the photoprotective efficacy. *J. Therm. Anal. Calorim.* **2022**, *147*, 7829–7836. [CrossRef]
56. Fan, W.; Zhu, W.; Zhang, X.; Xu, Y.; Di, L. Application of the combination of ball-milling and hot-melt extrusion in the development of an amorphous solid dispersion of a poorly water-soluble drug with high melting point. *RSC Adv.* **2019**, *9*, 22263–22273. [CrossRef] [PubMed]
57. Gong, N.; Wang, X.; Wang, Y.; Yang, S.; Song, J.; Lu, Y.; Du, G. Control over Polymorph Formation of Polydatin in Binary Solvent System and Structural Characterization. *J. Pharm. Biomed. Anal.* **2020**, *190*, 113260. [CrossRef]
58. Liu, B.; Li, Y.; Xiao, H.; Liu, Y.; Mo, H.; Ma, H.; Liang, G. Characterization of the Supermolecular Structure of Polydatin/6-O-α-Maltosyl-β-cyclodextrin Inclusion Complex. *J. Food Sci.* **2015**, *80*, C1156–C1161. [CrossRef]
59. Ao, F.; Shen, W.; Ge, X.; Wang, L.; Ning, Y.; Ren, H.; Fan, G.; Huang, M. Effects of the crystallinity on quercetin loaded the Eudragit L-100 electrospun nanofibers. *Colloids Surf. B Biointerfaces* **2020**, *195*, 111264. [CrossRef]
60. Moreira da Costa, E.; Maria Barbosa Filho, J.; Gomes do Nascimento, T.; Oliveira Macêdo, R. Thermal characterization of the quercetin and rutin flavonoids. *Thermochim. Acta.* **2002**, *392–393*, 79–84. [CrossRef]
61. Xin, M.; Ma, Y.; Lin, W.; Xu, K.; Chen, M. Study on the structure-activity of dihydromyricetin and its new production: Myricetin by using ESR and spectroscopic techniques. *J. Therm. Anal. Calorim.* **2014**, *116*, 241–248. [CrossRef]
62. Li, Y.L.; Yang, Y.; Bai, T.C.; Zhu, J.J. Heat capacity for the binary system of quercetin and poly(vinylpyrrolidone) K30. *J. Chem. Eng. Data* **2010**, *55*, 5856–5861. [CrossRef]
63. Höhne, G.W.H.; Hemminger, W.F.; Flammershein, H.-J. Applications of Differential Scanning Calorimetry. In *Differential Scanning Calorimetry*, 2nd ed.; Springer: Berlin/Heidelberg, Germany, 2003; pp. 147–152. [CrossRef]
64. *Measuring Specific Heat Capacities*; USER COM 7 TA TIP; Metller Toledo: Schwerzenbach, Switzerland, 1998.

Disclaimer/Publisher's Note: The statements, opinions and data contained in all publications are solely those of the individual author(s) and contributor(s) and not of MDPI and/or the editor(s). MDPI and/or the editor(s) disclaim responsibility for any injury to people or property resulting from any ideas, methods, instructions or products referred to in the content.